Tailoring Elastic Properties of Silica Aerogels Cross-Linked with Polystyrene

Baochau N. Nguyen,*,† Mary Ann B. Meador,*,‡ Marissa E. Tousley,§ Brian Shonkwiler,⊥ Linda McCorkle,† Daniel A. Scheiman,¶ and Anna Palczer‡

Ohio Aerospace Institute, 22800 Cedar Point Road, Brookpark, Ohio 44142, and NASA Glenn Research Center, 21000 Brookpark Road, Cleveland, Ohio 44135

ABSTRACT The effect of incorporating an organic linking group, 1,6-bis(trimethoxysilyl)hexane (BTMSH), into the underlying silica structure of a styrene cross-linked silica aerogel is examined. Vinyltrimethoxysilane (VTMS) is used to provide a reactive site on the silica backbone for styrene polymerization. Replacement of up to 88 mol % of the silicon from tetramethoxyorthosilicate with silicon derived from BTMSH and VTMS during the making of silica gels improves the elastic behavior in some formulations of the cross-linked aerogels, as evidenced by measurement of the recovered length after compression of samples to 25% strain. This is especially true for some higher density formulations, which recover nearly 100% of their length after compression to 25% strain twice. The compressive modulus of the more elastic monoliths ranged from 0.2 to 3 MPa. Although some of these monoliths had greatly reduced surface areas, changing the solvent used to produce the gels from methanol to ethanol increased the surface area in one instance from 6 to 220 m^2/g with little affect on the modulus, elastic recovery, porosity, or density.

KEYWORDS: aerogels • polystyrene • cross-linking • mesoporous materials • hybrid materials • elastic recovery

INTRODUCTION

Silica aerogels with their low density and thermal conductivity are potential candidates for various thermal, optical, and acoustic applications for aerospace including multipurpose structures for vehicles, space suits, and habitats (1). However, the use of aerogel monoliths has been restricted because of their inherent fragility, hygroscopic nature, and poor mechanical properties. It has been demonstrated that by cross-linking the skeletal structure of the silica gel through silanol groups on the surface with a diisocyanate, the strength is improved by as much as 2 orders of magnitude while only doubling the density over those of native or non-cross-linked aerogels (2). In addition, the mesoporosity of the cross-linked aerogels and hence their superior insulating properties, among other things, are maintained. Incorporating a functional group such as amine, vinyl, or free-radical initiator into a silica-based aerogel improves the cross-linking with isocyanates (3, 4) and also expands the types of organic monomers that can be used as cross-linkers to include epoxides (5) or styrene (6).

While the cross-linked aerogels are a great improvement over the native silica aerogels, for many applications it is most desirable to have a flexible material. Though some measure of flexibility is obtained in the cross-linked aerogels through a decrease in the density (4), it has been shown that more flexibility is obtained in non-cross-linked aerogels by alteration of the silica backbone in some significant way. For example, Kramer et al. (7) demonstrated that including up to 20% (w/w) poly(dimethylsiloxane) in tetraethoxyorthosilicate (TEOS)-based aerogels resulted in rubbery behavior with up to 30% recoverable compressive strain. More recently, Rao et al. (8) has demonstrated that utilizing methyltrimethoxysilane (MTMS) as the silica precursor and a two-step synthesis imparts extraordinary flexibility to the aerogels. The MTMS-derived aerogels are more flexible largely because of the resulting lower cross-link density of the silica [three alkoxy groups that can react versus four in rigid tetramethoxyorthosilicate (TMOS)- or TEOS-derived aerogels]. Kanamori et al. (9), using a surfactant to control the pore size and a slightly different process, have shown that MTMS-derived gels can be made that demonstrate reversible deformation on compression. In fact, some formulations were able to be dried ambiently, which exerts similar compressive forces on the gels. Initially, the gels shrink about 65% but spring back to nearly their original size, resulting in nearly the same density and pore structure as those dried supercritically.

In this study, we examine the effect of incorporating an organic linking group into the underlying silica structure to achieve the same effect. Shea and Loy have employed bridged bis(trialkoxysilyl) monomers as precursors for silsesquioxane-derived aerogels and xerogels (10). Typically, this allowed for control of the pore size directly related to the size of the bridge, with the best results obtained using a stiffer structure such as an arylene chain. More flexible bridges such as alkyl chains resulted in more compliant aerogels but tended to shrink more, reducing the porosity.

* To whom correspondence should be addressed. E-mail: Baochau.n.nguyen@nasa.gov (B.N.N.), maryann.meador@nasa.gov (M.A.B.M.).
Received for review November 3, 2008 and accepted January 29, 2009
† Ohio Aerospace Institute.
‡ NASA Glenn Research Center.
§ NASA LERCIP Summer Intern.
⊥ Present address: Clark Atlanta University, Atlanta, GA 30314.
¶ Employed by ASRC, Cleveland, OH 44135.
DOI: 10.1021/am8001617

To counteract this, we also apply the technology of using a conformal coating of polymer over the silica skeleton. In this way, we impart the same type of elastic properties as those seen with the MTMS-derived aerogels while also improving the mechanical strength of the aerogels. Hence, in this study, we replace some of the silicon derived from TMOS used in the preparation of the aerogels with those from 1,6-bis(trimethoxysilyl)hexane (BTMSH). Vinyltrimethoxysilane (VTMS) is also incorporated as a site for styrene cross-linking in these gels. A statistical experimental design is employed to examine the effect of four variables used in the preparation of the aerogels, including the total concentration of silicon (derived from TMOS, VTMS, and BTMSH combined), mol % of VTMS and BTMSH, and polystyrene formulated molecular weights (FMWs) on mechanical and other properties of the aerogels.

EXPERIMENTAL SECTION

General Procedures. Tetramethylorthosilicate (TMOS), tetraethylorthosilicate (TEOS), vinyltrimethoxysilane (VTMS), and bis(trimethoxysilyl)hexane (BTMSH) were purchased from Gelest, Inc. Ammonium hydroxide (NH_4OH; 28−30 wt % solution) and concentrated nitric acid were purchased from Fisher. Methanol (MeOH), ethanol (EtOH), chlorobenzene, styrene, 2,2′-azobis(2-methylpropionitrile) (AIBN), and acetone were purchased from Aldrich. All reagents were used without further purification.

Preparation of Silica Gels. Variables used in the preparation of aerogel monoliths are the concentration of total silicon in the total solution, VTMS and BTMSH mole fractions, and the formulated molecular weight (FMW) of polystyrene, as shown in Table 1. The amount of NH_4OH was kept constant at 1 mL for every 100 mL of the total volume of the final solution. The silica gels were prepared by combining an alcohol solution of the three silane components with water and catalyst. In a typical example, formulation 12 from Table 1 was made from 1.82 mol/L of total silicon having 29 mol % VTMS, 49 mol % BTMSH, and 22 mol % TMOS. A solution of 8.00 mL (52.48 mmol) of VTMS, 14.50 mL (45.00 mmol) of BTMSH, and 5.95 mL (39.56 mmol) of TMOS in 46.00 mL of MeOH was cooled to below 0 °C in an acetone/dried-ice bath. A basic solution consisting of 1.00 mL of NH_4OH and 24.55 mL of H_2O was then added to the silane mixture. The contents were thoroughly mixed together before being poured into 20-mL plastic syringe molds. Wet gels formed within 15 min to 2 h and were aged for 24 h. After aging, the gels were extracted into fresh MeOH and allowed to rest for 24 h before being rinsed again. Similar to formulation 12, formulation 17 was prepared under the same conditions but EtOH was used in place of MeOH. The solvent was then gradually exchanged with chlorobenzene.

A 50% (w/w) solution of styrene in chlorobenzene was prepared. The ratio of initiator, AIBN, to styrene monomer was used to control the final styrene FMW. For example, theoretically to obtain a styrene oligomer with FMW of 500 g/mol, an amount of 8.21 g (0.05 mol) of AIBN is dissolved in a solution of 50 g (0.48 mol) of styrene in 50 g of chlorobenzene. It should be noted that every 1 mol of AIBN produces 2 mol of free radical. All gels were soaked in the styrene mixture for 3 days, after which they were transferred to fresh chlorobenzene, followed by heat treatment at about 70−75 °C for 24 h. The polystyrene-cross-linked gels were washed with chlorobenzene twice before solvent exchange with acetone and dried using supercritical carbon dioxide (CO_2) extraction.

Instruments. The skeletal density (ρ_s) was measured using a Micromeritics Accupyc 1340 helium pycnometer. All samples were outgassed at 80 °C for 24 h under a vacuum. Samples for microscopy were coated with gold/palladium and viewed using a Hitachi S-4700-11 field emission scanning electron micro-

Table 1. Preparation Conditions and Measured Properties for Aerogels in the Study

formulation	total silicon, M	water/silicon ratio	VTMS, mol%	BTMSH, mol%	polystyrene FMW	gelation solvent	bulk density, g/cm^3	porosity, %	shrinkage, %	modulus, MPA	unrecovered strain, %	contact angle, deg	BET surface area, m^2/g	T_d, °C in N_2
1	1.49	8.5	20	30	1500	MeOH	0.327	76.78	25.0	17.54	9.50	133.4	576.37	278.37
2	1.25	7.7	40	48	2500	MeOH	0.175	85.90	10.0	0.47	1.55	125.1	8.12	266.50
3	1.68	8.7	42	0	500	MeOH	0.330	76.64	20.0	20.35	10.00	114.6	667.39	294.93
4	1.61	9.1	25	0	2500	MeOH	0.327	77.33	22.0	20.00	9.50	112.2	640.03	322.24
5	1.82	7.8	29	49	2500	MeOH	0.232	82.32	8.5	3.29	0.45	137.4	157.85	263.16
6	1.82	5.2	29	49	2500	MeOH	0.241	81.65	9.0	1.07	1.95	137.0	94.64	270.00
7	2.05	8.1	34	29	1500	MeOH	0.284	78.36	10.5	10.68	8.15	138.3	549.71	283.06
8	1.25	7.7	40	48	1500	MeOH	0.172	86.19	10.0	0.23	2.65	131.9	7.72	271.50
9	1.98	8.4	20	30	500	MeOH	0.370	70.58	20.0	32.43	11.10	127.0	750.69	279.93
10	1.06	8.1	47	28	500	MeOH	0.122	90.34	5.5	0.17	9.90	125.3	366.11	287.28
11	0.99	8.7	20	30	2500	MeOH	0.309	77.89	33.5	18.04	6.70	133.7	600.98	278.70
12	1.82	7.8	29	49	500	MeOH	0.243	81.15	8.5	2.42	1.00	127.4	6.06	274.30
13	1.82	5.2	29	49	500	MeOH	0.250	80.92	9.0	0.87	1.30	135.2	69.62	263.34
14	1.06	8.1	47	28	500	MeOH	0.125	90.33	6.5	0.20	8.40	132.2	372.24	279.47
15	1.25	7.7	40	48	2500	EtOH	0.197	84.70	13.0	1.45	8.30	130.9	310.70	305.7
16	1.25	7.7	40	48	1500	EtOH	0.210	83.66	15.5	1.44	9.75	134.0	276.89	305.5
17	1.82	7.8	29	49	500	EtOH	0.244	81.74	8.0	1.8	1.35	137.8	220.98	312.0

scope. Supercritical CO_2 fluid extraction was performed using an Applied Separations 1-L Spe-ed SFE-2 manual system. Mechanical tests were done on an Instron 4505 eletromechanical machine using Testworks 4 software and a 10 000 N load cell at 0.25/min. Nitrogen sorption measurements using the Brunauer–Emmett–Teller (BET) method were performed on a Micromeritics ASAP2020 chemisorption system, using N_2 gas. Solid ^{13}C and ^{29}Si NMR spectra were obtained on a Bruker Avance-300 spectrometer with a 4-mm solids probe using cross polarization and magic angle spinning at 11 kHz. The ^{13}C NMR spectra were externally referenced to the carbonyl of glycine, which appears at 176.01 ppm, and the ^{29}Si NMR spectra were externally referenced to the silicon of 3-(trimethoxysilyl)propionic acid, which is at 0 ppm. The hydrophobicity was determined by the contact angle of the water droplet on a flat surface of an aerogel, using a Rame goniometer with *Drop Image*, version 1.5.04. The flat surface was prepared by sanding of the aerogel with 400-grit silicon carbide sandpaper until smooth and flat surfaces were obtained. A minimum of three measurements was collected on one sample/formulation, and their average values are reported in Table 1.

The thermal degradation temperatures (T_d) of the cross-linked aerogels were measured using a Q500 thermal gravimetric analyzer from TA Instruments under N_2 gas. IR spectra were obtained using a Thermo Electron Corporation Nicolet 380 FT-IR with a germanium crystal and a single-pass attenuated total reflectance.

Characterization. The bulk density (ρ_b) was determined by measuring the weight and volume of the sample. Dimensional change, or shrinkage (%), is taken as the difference between the diameters of the aerogel monolith and of the 20-mL syringe mold (nominally 20 mm). The skeletal density from helium pycnometry (ρ_s) and the bulk density were used to calculate the porosity (%) of the aerogels using eq 1.

$$\text{porosity } \% = \frac{1/\rho_b - 1/\rho_s}{1/\rho_b} \times 100 \qquad (1)$$

Compression tests were carried out on the aerogel monoliths in two steps. First, the aerogels were compressed to 25% strain. The test was stopped, the crosshead was instantly moved back to zero, and the procedure was repeated once more and released. The specimen was then left to sit for 30 min at room temperature. At that time, the final thickness was measured and the unrecoverable strain (%) was calculated as a percentage of the initial length that did not recover. The modulus was taken as the initial slope from the stress–strain curve of the first compression.

Statistical Analysis. Experimental design and analysis was conducted using Design Expert 7.1.3 available from Stat-Ease, Inc. Using a d-optimal design to minimize the number of experiments, a total of 17 distinct batches of polystyrene cross-linked aerogels were prepared by varying the total silicon concentration (0.99–2.05 mol/L), the fraction of silicon derived from VTMS (20–47 Si mol %) and BTMSH (0–49 Si mol %), and the polystyrene FMW used as a cross-linker (500–2500 FMW). The silicon concentration and silicon mole percent were used in this study instead of the silane concentration because every 1 mol of BTMSH contributes 2 mol of silicon while TMOS and VTMS contribute 1 mol of silicon each. Preparation conditions and measured properties of all of the aerogels are listed in Table 1. The number represents a particular formulation made at once in a single batch. Using statistical design of experiment, the order of the preparation of individual formulations is random to reduce the correlation of systematic errors with any variable.

Formulations 1–14 shown in Table 1 were modeled using multiple linear least-squares regression analysis, considering a model including all first-order effects of the four variables, as well as all two-way interactions (11). All of the variables were orthogonalized (transformed to a −1 to +1 scale) prior to modeling to minimize correlation among terms. Terms not statistically significant (<90% confidence) were dropped from the model one at a time by the backward stepwise modeling technique. Summary statistics and significant terms in the models are shown in Table 2.

Table 2. Summary Statistics and Significant Terms for the Empirical Models

response	significant terms in model	standard error	R^2
density	total silicon, VTMS, BTMSH, styrene	0.004 g/cm^3	0.999
	total silicon * BTMSH		
	total silicon * styrene		
	VTMS * BTMSH		
shrinkage	total silicon, VTMS, BTMSH, styrene	0.68%	0.997
	total silicon * VTMS		
	total silicon * BTMSH		
	BTMSH * styrene		
porosity	total silicon, VTMS, BTMSH, styrene	0.25%	0.999
	total silicon * BTMSH		
	total silicon * styrene		
	VTMS * BTMSH		
	VTMS * styrene		
	BTMSH * styrene		
modulus (log)	total silicon, VTMS, BTMSH	0.76	0.881
unrecovered strain (log)	BTMSH, BTMSH(2)	0.38	0.899
onset of decomposition	BTMSH, styrene, BTMSH * styrene	1.44 °C	0.925

RESULTS AND DISCUSSION

Styrene cross-linked aerogels listed in Table 1 were prepared by first reacting a mixture of TMOS, VTMS, and BTMSH with a base catalyst to form a backbone with a structure as shown in Scheme 1. As indicated, increasing amounts of BTMSH and VTMS in place of TMOS effectively reduce the size of pure silica regions in the gel and result in a more open, flexible backbone structure. In addition, because of slower reaction rates compared to TMOS as well as the availability of only three siloxyl bonding sites, the vinyl- and hexyl-containing silicon will tend to be on the surface of the primary particles. Subsequent cross-linking with styrene is expected to proceed according to Scheme 2, where a certain ratio of AIBN to styrene (vide infra) is used to promote cross-links varying in size between 500 and 2500 g/mol.

The water/silicon mole ratio used to make the gels before cross-linking is calculated based on the number of moles of water over the total moles of silicon. According to Brinker and Scherer (12), incomplete hydrolysis of silane precursors occurs when the water to silicon ratio, r, is low. Because water is a byproduct of condensation, an r of 2 is stoichiometric for complete hydrolysis and condensation. In most of the formulations from this study, r ranged from 7.7 to 9.1 (large excess of water), but in some formulations (2, 5, 8, and 12), where BTMSH-derived silicon is close to 50 mol %,

Scheme 1. Proposed Molecular Structure of Silica Gel Made from Approximately 28% VTMS and 40% BTMSH

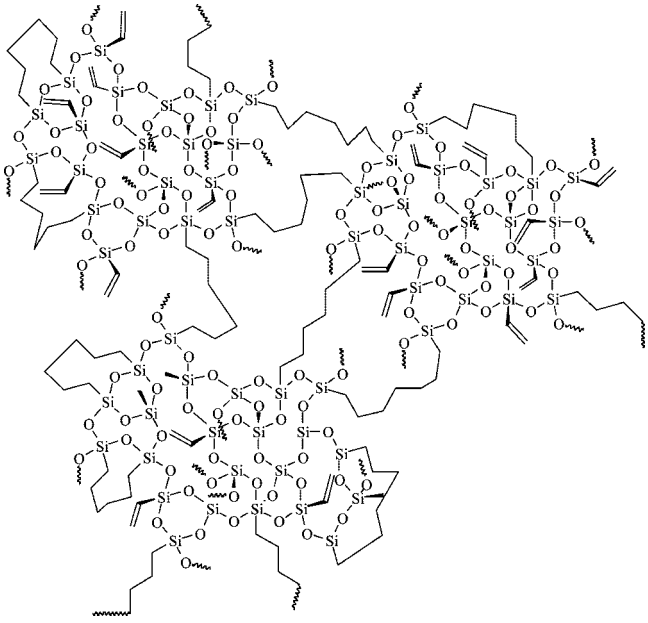

Scheme 2. Proposed Cross-Linking with VTMS and Styrene

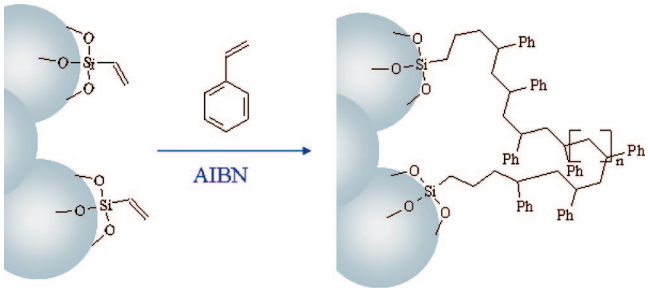

the high water content caused the silane mixture to cloud up and start to form emulsions. This was most likely due to the increased content of hydrophobic hexyl and vinyl groups as the concentration of TMOS became very small. To attempt to solve this problem, the water level for two formulations (5 and 12) was adjusted and remade as formulations 6 and 13, respectively, until a clearer, more homogeneous solution was achieved (r = 5.2). However, the resulting aerogels looked the same (white and opaque), and as shown in Table 1, the bulk properties of the resulting monoliths did not change much with the change in the water concentration.

In formulations prepared from MeOH in which the solubility and inhomogeneity of the gels become an issue, the biggest consequence is the loss of mesoporosity in the resulting monoliths. This is evidenced by BET surface areas, which ranged from 6 to 160 m^2/g for formulations where BTMSH-derived silicon was close to 50 mol %. In contrast, for formulations where BTMSH-derived silicon is at or below 30 mol %, surface areas ranged from 360 to 670 m^2/g. To illustrate, four micrographs of selected monoliths are shown in Figure 1. Monoliths pictured in Figure 1a, prepared using no BTMSH, and in Figure 1b, with 29 mol % BTMSH-derived silicon, have the smallest particle sizes, small uniform pores,

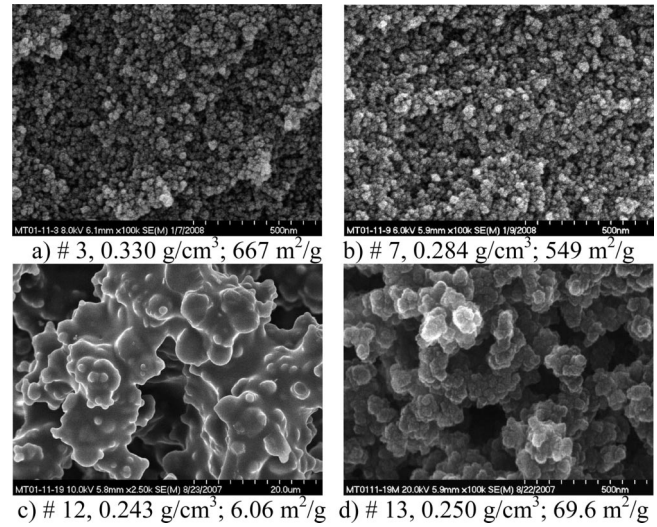

FIGURE 1. Scanning electron micrographs of selected samples from a study with the density and surface labeled.

and high surface areas. In contrast, the micrograph of the monolith from formulation 12 shown in Figure 1c, prepared with 49 mol % silicon from BTMSH, has very large feature sizes, noting that the micrograph is taken at a vastly different scale than the others. Reduced water in the initial sols does result in a reduction in the particle and pore sizes and an increase in the surface area somewhat, as shown in Figure 1d for monoliths prepared according to formulation 13 in comparison to that shown in Figure 1c for those from formulation 12.

It was found that the phase separation issue (and concomitant reduction in the surface area) can be better resolved by changing the solvent from MeOH to EtOH. To illustrate, a few formulations with the BTMSH concentration close to 50 mol % were made using EtOH as the gelation solvent (formulations 15–17). EtOH, being a less polar solvent than MeOH and having a higher alkyl chain, better solvates the vinyl and hexyl groups on the surface of the developing silica particles, thus keeping a more homogeneous or continuous phase. This results in clearer sols even though the water to silicon ratio remains the same (r = 7.7–7.8). In comparison to the same formulations made with MeOH (formulations 2, 8, and 12, respectively), only slight changes in the density and porosity are observed. However, dramatic changes in the microstructure are obtained by changing the solvent from MeOH to EtOH, as evidenced by micrographs shown in Figure 2a–f. The pairs of formulations shown in parts a (2) and b (15), c (8) and d (16), and e (12) and f (17) of Figure 2 differ only in the gelation solvent. It is clear from the micrographs that formulations prepared in EtOH have a more uniform, finer particle structure than those prepared in MeOH. Even more dramatic, the surface areas for the EtOH formulations range from 220 to 311 m^2/g compared to from 6 to 8 m^2/g for those prepared in MeOH.

The aerogels were also characterized using ^{29}Si and ^{13}C NMR and FT-IR. FT-IR spectra of the monoliths indicate that not all vinyl groups are consumed in the reaction with polystyrene. Although the CH peak from unreacted vinyl at

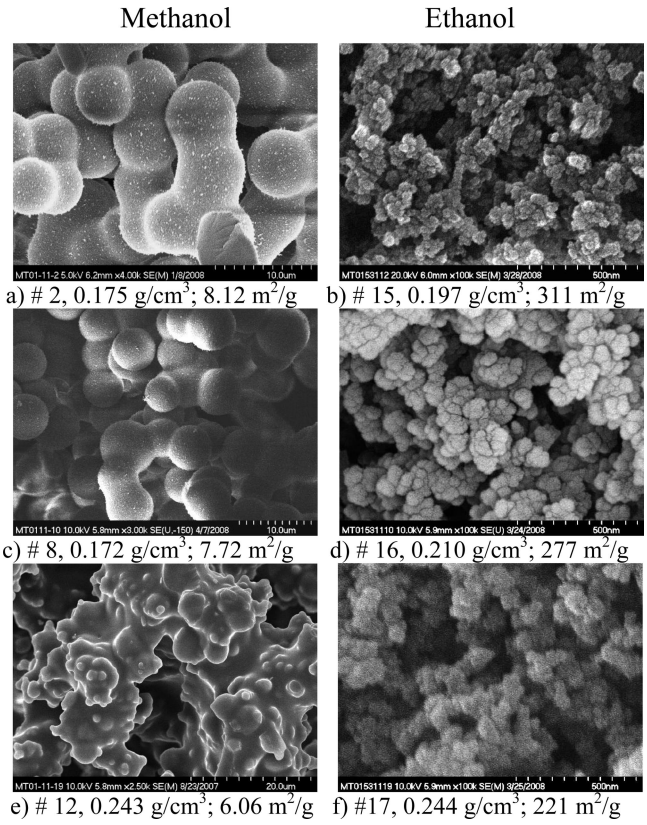

FIGURE 2. Scanning electron microscopy images of aerogel monoliths prepared from (left) a MeOH solution and (right) an EtOH solution. Monoliths pairs (a) 2 and (b) 15, (c) 8 and (d) 16, and (e) 12 and (f) 17 differ only in the gelation solvent.

1000 cm^{-1} (out-of-phase deformation) partially overlaps the Si−O−Si peak at 1100 cm^{-1}, its absorbent intensity increases with an increase in the amount of BTMSH. Representative ^{13}C NMR spectra are shown in Figure 3. In Figure 3a, from aerogels prepared with no BTMSH and 42 mol % VTMS-derived silicon (formulation 3), the aromatic carbons of polystyrene appear at 129 and 146 ppm while the broad peak at 40 ppm can be assigned to the aliphatic carbons resulting from the copolymerization of styrene and vinyl present on the silica gel surface. The small peak at 135 ppm can be assigned to one of the two vinyl carbons from VTMS that has not reacted. (The other unreacted vinyl peak is masked by the styrene aromatic peak at 129 ppm.) In contrast, Figure 3b shows a spectrum of a monolith prepared in formulation 7, where 29 mol % of total silicon are derived from BTMSH and 40 mol % come from VTMS. The aromatic styrene peaks are still present, but the aliphatic peaks are masked by the presence of peaks at 12, 22, and 32 ppm due to the methylene groups from BTMSH and a residual methoxy peak at 51 ppm. In addition, the peak at 135 ppm is much larger, indicating that more unreacted vinyl is present. Figure 3c shows a spectrum from a monolith prepared in formulation 2 where BTMSH-derived silicon is increased to 48 mol % of total silicon and 40 mol % come from VTMS. In this formulation, little styrene polymerization is evident judging from the very small resonances at 148 and 40 ppm. Indeed, only peaks due to unreacted vinyl (129 and 135 ppm), methylenes from BTMSH (12, 22, and 32 ppm), and

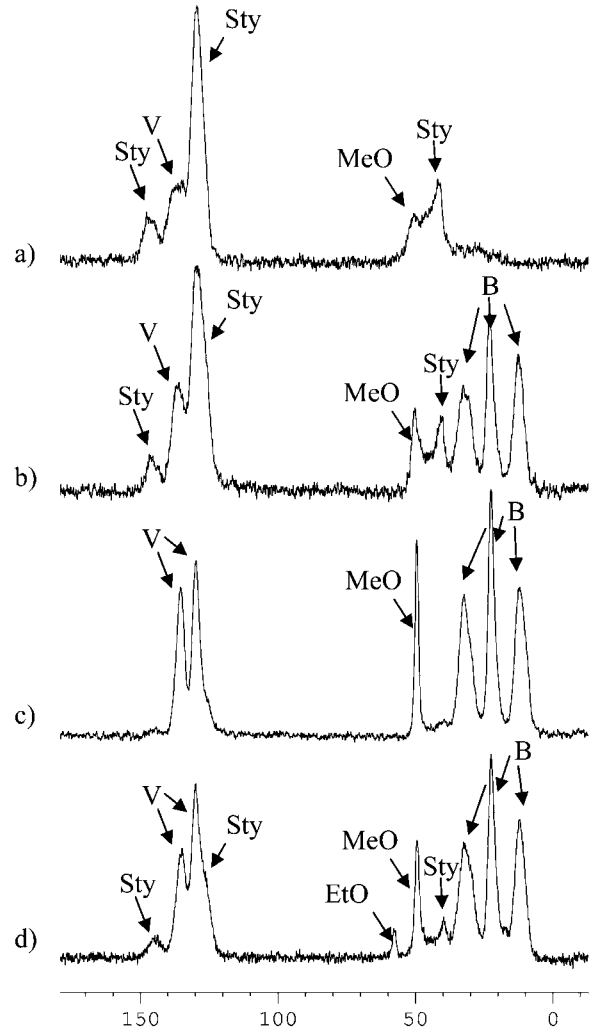

FIGURE 3. Solid ^{13}C NMR of samples from formulations (a) 3 with no BTMSH, (b) 7 with 29% BTMSH, (c) 2 with 48% BTMSH prepared in a MeOH solution, and (d) 15, same as 2 but prepared in EtOH (Sty = styrene peaks, B = BTMSH peaks, V = vinyl peaks).

residual methoxy are evident in the spectrum. Similar results were obtained in all MeOH-derived formulations, where BTMSH contributed nearly 50 mol % of total silicon.

The polymer-poor effect may be partially due to the vinyl sites from VTMS being sterically blocked by hexyl links from BTMSH, as shown in the proposed molecular structure in Scheme 1 with about 40 mol % of the silicon atoms being derived from BTMSH and 28 mol % from VTMS. In addition, the greatly reduced surface areas in monoliths where BTMSH is high will also reduce the availability of vinyl groups for cross-linking. This is evidenced by the increased amount of styrene cross-linking in formulation 15, prepared in EtOH, whose NMR spectrum is shown in Figure 3d. Monoliths from this formulation have a surface area of 311 m^2/g, compared to that of formulation 2 (8 m^2/g), whose spectrum is shown in Figure 3c.

Even though a large enough excess of water was used in all cases, evidence of incomplete hydrolysis of the methoxy group (−OCH_3) from the silane precursor(s) is observed by the large methoxy peaks at 51 ppm seen in the ^{13}C NMR spectrum, in Figure 3a−d. This −OCH_3 peak becomes more

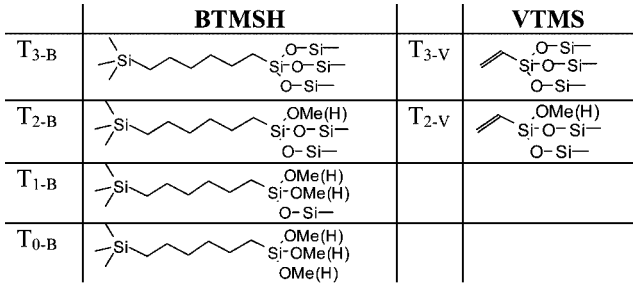

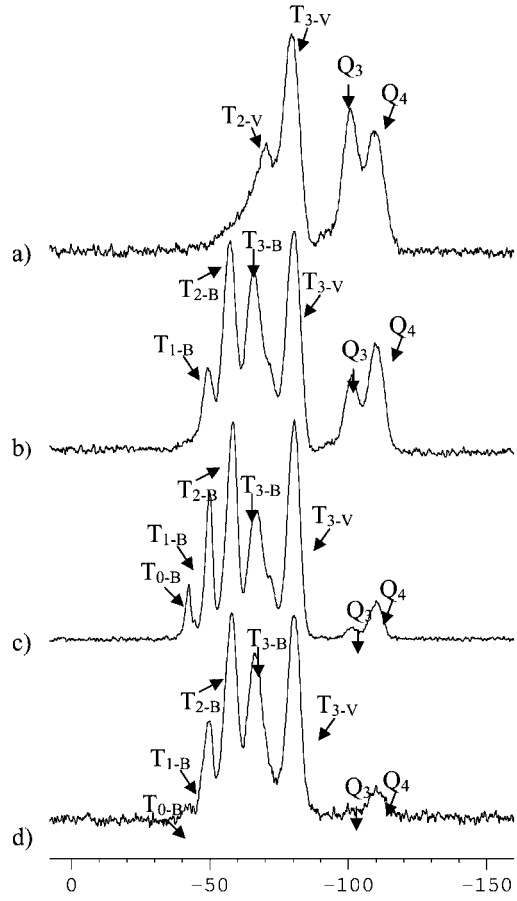

FIGURE 4. Solid ^{29}Si NMR of samples from formulations (a) 3 with no BTMSH, (b) 7 with 29% BTMSH, (c) 2 with 48% BTMSH prepared in a MeOH solution, and (d) 15, same as 2 but prepared in EtOH.

intense at higher concentrations of total silicon as well as in higher mole fractions of BTMSH. Similar observations of incomplete hydrolysis and condensation are also seen in ^{29}Si NMR shown in Figure 4. Figure 4a shows the spectrum for monoliths from formulation 3, where no BTMSH is used. Two broad peaks are observed for the VTMS-derived silicon, a peak at −80 ppm (T_3 peak) and at −70 ppm (T_2 peak). The peak at −70 ppm integrates to about one-third of the area of the −80 ppm peak, indicating that only about three-quarters of the vinyl silicon atoms are completely reacted. TMOS-derived silicon appears at −110 ppm (Q_4 peak) and −100 ppm (Q_3 peak). In spectra shown in Figures 4b–d, where BTMSH-derived silicon in the monoliths ranged from 29 to 49 mol %, the same VTMS- and TMOS-derived peaks are in evidence. In addition, up to four broad peaks are shown for BTMSH-derived silicon. Fully reacted BTMSH-derived silicon (T_3) appears at −67 ppm, while the T_2 peak appears at −58 ppm and the T_1 peak appears at −49 ppm. The small Si peak at −42 ppm (T_0 peak with three residual hydroxyl or methoxy groups) is observed for hexyl-linked disilanes that have reacted on only one side. The bottom two spectra correspond to formulations 2 (Figure 4c) and 15 (Figure 4d), which differ only in the solvent used for gelation. Peaks at −42 and −49 ppm appear to be smaller and the peak at −67 ppm appears larger in Figure 4d, indicating that the EtOH-prepared monoliths from formulation 15 have a slightly higher degree of reaction for BTMSH-derived silicon compared to the MeOH-prepared monoliths from formulation 2. The same observation is seen for all EtOH-derived monoliths compared to their MeOH counterparts.

Density, Dimensional Change, and Porosity. Empirical models for the density, dimensional shrinkage, and porosity for formulations 1–14 shown in Table 1 were derived, using multiple linear least-squares regression analysis. A full quadratic model was considered. Plots of the empirical models are shown in Figure 5a–f.

All four variables have a statistically significant effect on the density, as shown in Figure 5a (22 mol % VTMSH) and Figure 5b (40 mol % VTMS), with the strongest effect being a large increase in the density with an increase in the total silicon concentration. Obviously, increasing the total silicon concentration provides a denser silica backbone, but it also may increase the density by increasing the amount of available vinyl sites for cross-linking even when the fraction of total silicon derived from VTMS is constant. One would expect an increase in the density with an increase in the BTMSH fraction simply because of the added weight of the hexyl groups. However, this is only true when when the total silicon concentration is low (1.0 mol/L). When the total silicon concentration is 2.0 mol/L, increasing BTMSH fraction causes a decrease in the density. This might be partially due to the previous observation that high amounts of BTMSH decrease the amount of styrene cross-linking by reducing the availability of vinyl possibly by steric interactions and by reducing the available surface area. This effect is especially true when the VTMS fraction is at 40 mol % (Figure 5b), where the measured surface areas in all cases are less than 10 m^2/g.

Of course, the density is also influenced by dimensional shrinkage over the course of processing of the aerogels. Shrinkage models are shown in Figure 5c (22 mol % VTMS) and Figure 5d (40 mol % VTMS). Overall, the VTMS fraction and polystyrene FMW have the greatest effect on shrinkage. A high VTMS fraction and a high polystyrene FMW reduce shrinkage by reinforcing the silica backbone through an increase in the amount of polymer cross-linking. On the other hand, low shrinkage is also observed when the total silicon concentration is high and the fraction of BTMSH-derived silicon is high. This is most likely due to the effect of the phase separation occurring most in these formulations, making the silica backbone and the pore sizes larger and, thus, less prone to collapse.

As expected, empirical models shown in Figure 5e (22 mol % VTMS) and Figure 5f (40 mol % VTMS) indicate that the porosity increases with a decrease in the silicon concen-

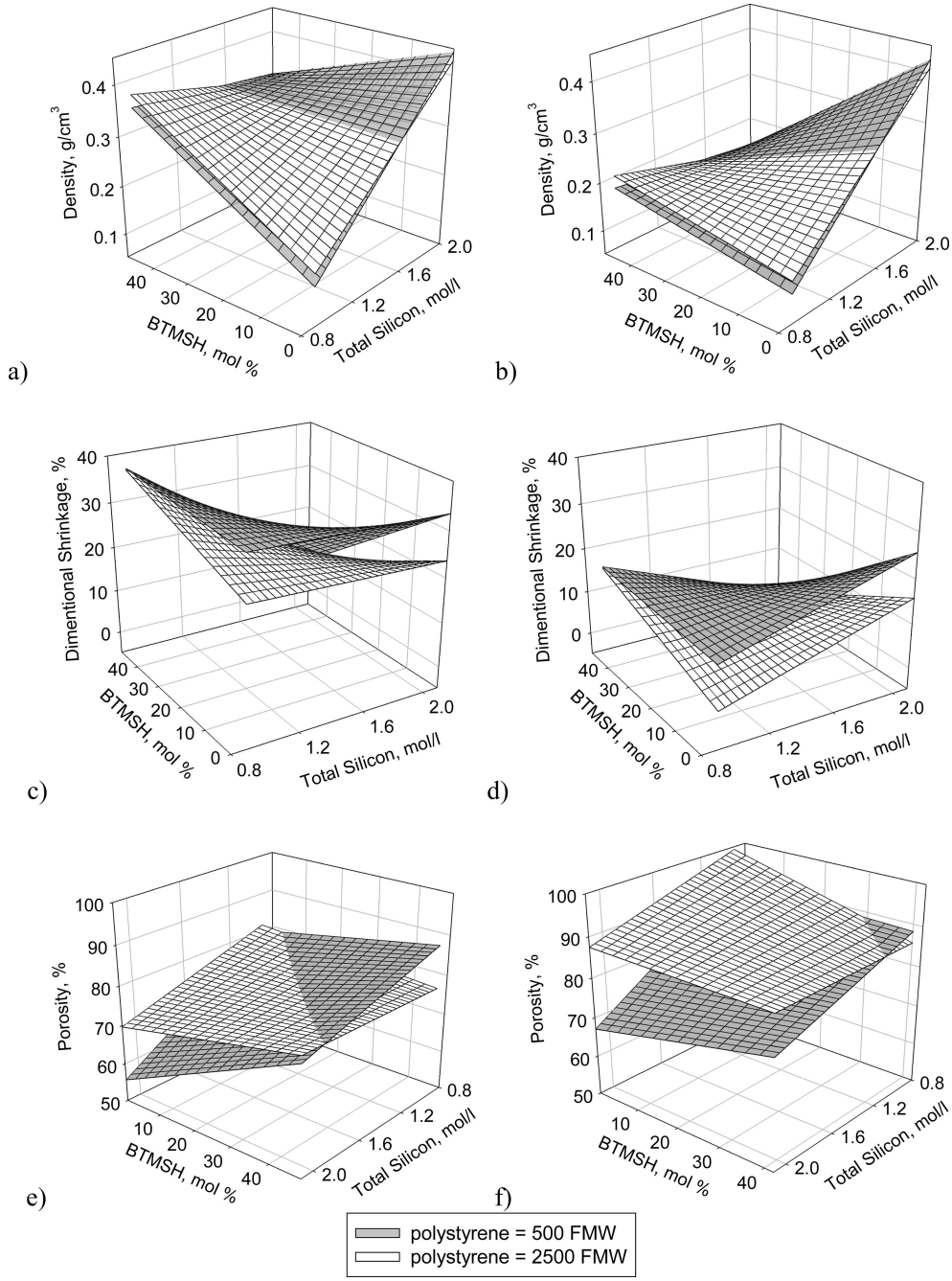

FIGURE 5. Response surface models for the density of aerogel monoliths versus mole percent of silicon from BTMSH and the total silane concentration using (a) 22 mol % VTMS and (b) 40 mol % VTMS, shrinkage (dimensional change) using (c) 22 mol % VTMS and (d) 40 mol % VTMS, and porosity using (e) 22 mol % VTMS and (f) 40 mol % VTMS.

tration and an increase in the vinyl groups, a trend opposite to that shown for the density. At high total silicon concentration, increasing the BTMSH fraction increases the porosity while at low total silicon concentration, it has only a minor effect on the porosity. These trends are more pronounced when the styrene FMW is 500. At higher polystyrene FMW, the empirical models are much flatter, indicating a smaller effect of total silicon concentration and vinyl content on the porosity. The highest porosities across the board are obtained when the polystyrene FMW is high and BTMSH and VTMS are also high, the conditions that give the least dimensional shrinkage.

Mechanical Properties. The modulus from compression tests was also modeled using multiple linear regression analysis, as shown in Figure 6. Only three of the main effects, the total silicon concentration, VTMS fraction, and BTMSH fraction were significant terms in the model. The styrene FMW was not significant over and above random error. As expected, the modulus increases with an increase in the total silicon concentration because this leads to higher densities. Surprisingly, the modulus decreases with an increase in the VTMS mole percent, even though this increases the number of sites available for cross-linking. However, increasing VTMS also tends to make the silica backbone less

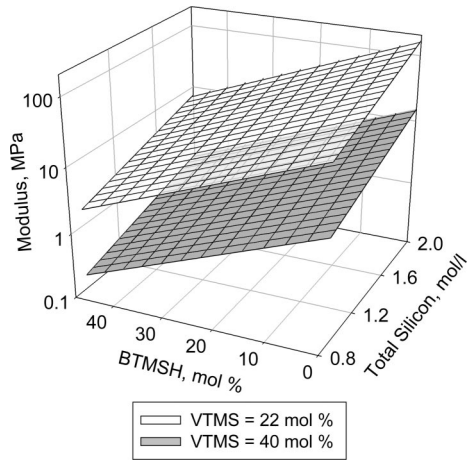

FIGURE 6. Response surface model for the modulus plotted versus the total silicon concentration and BTMSH-derived silicon mole percent.

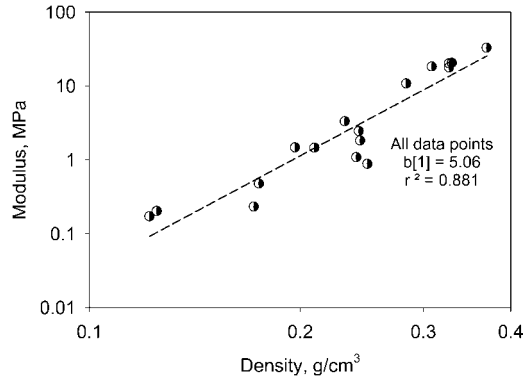

FIGURE 7. Power law dependency between the density and compressive modulus for all formulations including EtOH-derived aerogels.

stiff because of less siloxyl bonding. As expected, increasing the BTMSH silicon mole percent leads to decreases in the modulus, likely because of the effect of introducing more flexible links into the silica backbone but also because of the fact that at very high loadings the hexyl groups inhibit cross-linking.

The power law dependency between the density and compressive modulus for all formulations in the study (including EtOH formulations) is shown in Figure 7 with an exponent $b[1] = 5.06$ ($r^2 = 0.88$). Power law relationships between the modulus and density for native silica aerogels are typically reported with an exponent of 3−3.7 depending on the synthesis route (13) and have been shown to depend most on the connectivity between particles (14). It has also been reported that the power law dependency between the density and modulus for silica aerogels cross-linked with isocyanate is higher (3.99 for base-catalyzed, cross-linked aerogels) than that for native silica aerogels, possibly because the lower-density, conformal coating of the polymer reinforces the structure more efficiently by increasing the neck regions between particles (15). The greater increase in the exponent for the polystyrene cross-linked aerogels in this study may be due to the greater structure variation possible in this system and the fact that the amount of the total silicon concentration, fraction of silicon derived from VTMS and BTMSH, and amount of cross-linking all contribute to the density and modulus in different ways. It is clear, however, that the use of organic cross-linking leads to a higher modulus at lower density than using silica alone.

As a way of measuring the elastic properties, aerogel monoliths in the study were taken through two successive compression cycles to 25% strain. Two sample stress−strain curves from these tests are shown in Figure 8a (formulation 5) for a monolith with a high degree of recovery after compression (low unrecovered strain) and in Figure 8b (formulation 10) for a monolith with a lower degree of recovery. Note how the first and second compression curves nearly retrace each other in Figure 8a, while in Figure 8b, the second curve does not start to rise until about 13% strain. This amount represents the lost sample length after the first compression. Figure 9 shows a picture of the aerogel monolith made from formulation 5 before the test and after two compression cycles, showing that the sample length has changed very little through the course of the test.

The amount of unrecovered strain reported in Table 1 is a measure of the final length of the sample measured 30 min after the second compression compared to the length before compression. Only monoliths made with 48−49 mol % of silicon derived from BTMSH show a high degree of recovery (0.45−1.55% unrecovered strain for MeOH-derived formulations). As previously described, most of these formulations had low surface areas (more like a foam) and very little styrene cross-linking. The finding also indicates that good recovery is mainly governed by the amount of hexyl groups from BTMSH, as expected.

Of the formulations made in EtOH with high BTMSH, only one formulation (formulation 17) had a high degree of elastic recovery similar to the same formulation made in MeOH (formulation 12). Modulus was also relatively unchanged between the two formulations (1.8 MPa compared to 2.4 MPa). That result combined with a relatively large surface area (221 m^2/g) compared to aerogels made using formulation 12 makes aerogels from 17 perhaps the best formulation from the study, having both good elastic recovery and a higher surface area, which should lead to lower thermal conductivity. In the other EtOH-fabricated formulations (15 and 16), the modulus increased by a factor of 3−5 over the same formulations made in MeOH, but unrecovered strain was much higher. Monoliths from formulations 15 and 16 were made with a lower concentration of total silicon than formulation 17, which would tend to decrease the modulus, but a higher styrene FMW and a larger fraction of VTMS, both of which would result in a higher amount of styrene cross-linking. It would be of interest to examine the effect of the EtOH solvent on the other formulations with high BTMSH to further understand the effect of the total silicon concentration, styrene FMW, and VTMS on elastic recovery when phase separation is not as much of an issue.

Hydrophobicity. We have previously reported cross-linking aerogels with polystyrene by co-reacting with styrene bonded to the silica surface (6a). That method is more time-consuming than the vinyl route presented herein, having the

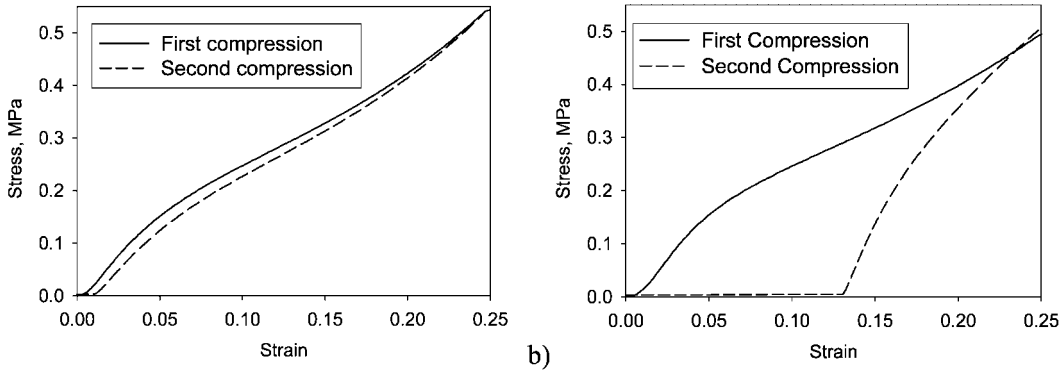

FIGURE 8. Typical stress−strain curves for repeat compression tests on (a) formulation 5 with 49 mol % BTMSH and (b) formulation 10 with 28 mol % BTMSH.

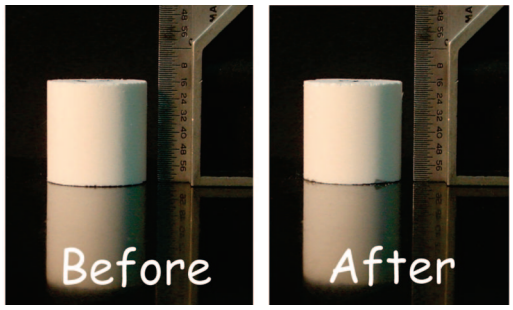

FIGURE 9. Monolith from formulation 5 shown before and after two compression cycles. The sample length decreased by less than 0.5% over the test.

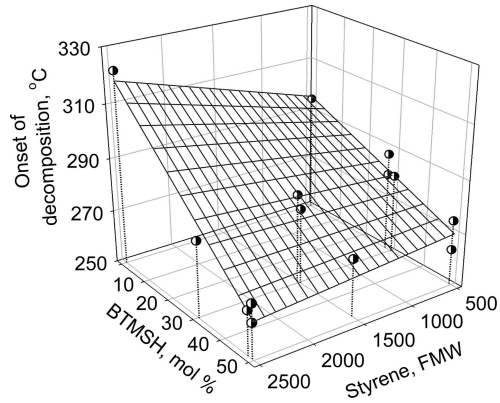

FIGURE 10. Graph of the response surface model for degradation temperature, T_d, of aerogel monoliths versus mole percent of BTMSH-derived silicon and FMW of polystyrene.

additional step of converting surface amines with *p*-chloromethylstyrene to provide the surface site for free-radical polymerization. Nevertheless, the polystyrene cross-linked aerogels previously reported were, as expected, found to be relatively hydrophobic (water droplet contact angle = 121.4°) compared to diisocyanate cross-linked aerogels (59.7°). Recently, Leventis et al. (6b) reported a new method of styrene cross-linking utilizing surface-initiated, free-radical polymerization by including a derivative of AIBN within the silica network. Despite the novel concept of this approach, the silane derivative of AIBN has a short shelf-life, and thus it must be prepared fresh from a lengthy and expensive synthetic route and stored at 10 °C before use. Nevertheless, the approach yielded styrene cross-linked aerogel monoliths with contact angles of 114.1°.

As listed in Table 1, contact angles measured in this study ranged from 112–114° on samples with no BTMSH silicon in agreement with those previously reported by Leventis. For samples with at least 29 mol % BTMSH silicon, contact angles were measured to be 127–138°. This indicates that the hexyl group from BTMSH is present on the silica surface and has a significant effect on the hydrophobic nature of the aerogels above and beyond the styrene cross-linking. The formulations prepared in EtOH (15−17) all exhibit higher contact angles compared to their MeOH counterparts (2, 8, and 12), suggesting that fewer residual methoxy groups and more complete condensation, as observed by NMR, have an effect on the hydrophobicity, as does the higher amount of styrene cross-linking.

Thermal Analysis. The temperature onset of thermal degradation (T_d) for all of the monoliths was measured by thermogravimetric analysis and is listed in Table 1. A response surface model shown in Figure 10, graphed along with data points, indicates that only the polystyrene FMW and BTMSH fraction have an effect on T_d over and above random error. Not surprisingly, the onset of decomposition is shown to decrease with an increase in the BTMSH fraction because the hexyl links in the underlying silica backbone are less stable than the pure silica. T_d's for polystyrene formulated at 500, 1500, and 2500 g/mol were measured to be 333, 347, and 350 °C, respectively. In agreement with this observation, increasing the polystyrene FMW is seen to increase the onset of decomposition by about 25 °C when no BTMSH is present. Increasing FMW has a negligible effect when the BTMSH fraction is high, probably because there is so little polystyrene cross-linking in these monoliths and also because the hexyl group from BTMSH is less stable than that from polystyrene. It should also be pointed out that, as the solvent is changed from MeOH to EtOH, the onset of decomposition of the aerogels increases over their MeOH counterparts, perhaps because of more complete condensation and fewer residual methoxy groups than the silane precursors. This is consistent with the observation from NMR that hydrolysis and condensation increase in EtOH-derived aerogels, leading to more stable structures.

CONCLUSIONS

The incorporation of flexible links in the underlying silica of aerogels cross-linked with polystyrene through vinyl

surface groups was examined. It was found that incorporation of the hexyl links from BTMSH improves elastic recovery after compression to 25% strain in the resulting monoliths. The inclusion of BTMSH also leads to more hydrophobicity of the aerogels, significantly increasing the contact angle of the monoliths compared to those having no BTMSH. The morphology of the monoliths was also shown to be dependent somewhat on the water to silane (or *r*) ratio and even more so on the solvent used to make the initial gels (MeOH vs EtOH). When MeOH was used as the solvent for formulations containing large fractions of silicon derived from BTMSH, poor solubility of the developing silica particles and phase separation results in extremely low surface areas, as measured by BET and large feature sizes observed by a scanning electron micrograph. Results obtained from ^{13}C NMR and FT-IR spectra suggested that this phase separation makes the vinyl sites from VTMS less available for cross-linking. Changing to EtOH as the solvent in some of these formulations both improved the homogeneity in the sols and increased the surface areas, as well as the hydrophobicity, in the final monoliths. Finally, a formulation (17) has been identified that gives a good combination of high surface area, porosity greater than 80%, a high degree of hydrophobicity, and excellent elastic recovery from compression with a modulus of almost 2 MPa, making it a candidate for use as a durable insulation for aerospace applications.

Acknowledgment. Financial support from NASA's Fundamental Aeronautics Program is gratefully acknowledged.

REFERENCES AND NOTES

(1) (a) Jones, S. M. *J. Sol–Gel Sci. Technol.* **2006**, *40*, 351–357. (b) Fesmire, F. E. *Cryogenics* **2006**, *46*, 111–117. (c) Pierre, A. C.; Pajonk, G. M. *Chem. Rev.* **2002**, *102*, 4243–4265.

(2) Zhang, G.; Dass, A.; Rawashdeh, A.-M. M.; Thomas, J.; Counsil, J. A.; Sotiriou-Leventis, C.; Fabrizio, E. F.; Ilhan, F.; Vassilaras, P.; Scheiman, D. A.; McCorkle, L.; Palczer, A.; Johnston, J. C.; Meador, M. A. B.; Leventis, N. *J. Non-Cryst. Solids* **2004**, *350*, 152–164.

(3) Meador, M. A. B.; Capadona, L. A.; McCorkle, L.; Papadopoulos, D. S.; Leventis, N. *Chem. Mater.* **2007**, *19*, 2247.

(4) Capadona, L. A.; Meador, M. A. B.; Alunni, A.; Fabrizio, E. F.; Vassilaras, P.; Leventis, N. *Polymer* **2006**, *47*, 5754.

(5) Meador, M. A. B.; Fabrizzio, E. F.; Ilhan, F.; Dass, A.; Zhang, G.; Vassilaras, P.; Johnston, J. C.; Leventis, N. *Chem. Mater.* **2005**, *17*, 1085.

(6) (a) Ilhan, U. F.; Fabrizzio, E. F.; McCorkle, L.; Scheiman, D. A.; Dass, A.; Palczer, A.; Meador, M. A. B; Johnston, J. C.; Leventis, N. *Mater. Chem.* **2006**, *16*, 3046. (b) Mulik, S.; Sotiriou-Leventis, C.; Churu, G.; Lu, H.; Leventis, N. *Chem. Mater.* **2008**, *20* (15), 5035–5046.

(7) Kramer, S. J.; Rubio-Alonso, F.; Mackenzie, J. D. *Mater. Res. Soc. Symp. Proc.* **1996**, *435*, 295–299.

(8) Rao, A. V.; Bhagat, S. D.; Hirashima, H.; Pajonk, G. M. *J. Colloid Interface Sci.* **2006**, *300*, 279.

(9) Kanamori, K.; Aizawa, M.; Nakanishi, K.; Hanada, T. *Adv. Mater.* **2007**, *19*, 1589–1593.

(10) Shea, K. J.; Loy, D. A. *Chem. Mater.* **2001**, *13*, 3306.

(11) Formulations 15–17 made from EtOH were not used in the modeling. It is obvious that changing the solvent from MeOH to EtOH has a real and dramatic effect on some properties of the monoliths, but not enough formulations in EtOH were completed to include the gelation solvent as a variable. For the same reason, *r* (ratio of water to silane) is not considered as a factor in the modeling, although it no doubt has an effect on some of the properties. In any case, including the effects of *r* and the gelation solvent in future analyses will only strengthen the relationships described herein.

(12) Brinker, C. J. and Scherer, G. W. *Sol–Gel Science: The Physics and Chemistry of Sol–Gel Processing*; Academic Press, Inc.: San Diego, CA, 1990.

(13) For example, see: (a) Pekala, R. W.; Hrubesh, L. W.; Tillotson, T. M.; Alviso, C. T.; Poco, J. F.; LeMay, J. D. *Mater. Res. Soc. Symp. Proc.* **1991**, *207*, 197–200.

(14) Woignier, T.; Reynes, J.; Hafidi Alaoui, A.; Beurroies, I.; Phalippou, J. *J. Non-Cryst. Solids* **1998**, *241*, 45–52.

(15) Zhang, G.; Dass, A.; Rawashdeh, A.-M. M.; Thomas, J.; Counsil, J. A.; Sotiriou-Leventis, C.; Fabrizio, E. F.; Ilhan, F.; Vassilaras, P.; Scheiman, D. A.; McCorkle, L.; Palczer, A.; Johnston, J. C.; Meador, M. A.; Leventis, N. *J. Non-Cryst. Solids* **2004**, *350*, 152–164.

AM8001617